



Transients and tradeoffs of phenotypic switching in a fluctuating limited environment

E. Filiba, D. Lewin, N. Brenner*

Department of Chemical Engineering, Technion, Israel

ARTICLE INFO

Article history:

Received 11 February 2012

Available online 26 June 2012

Keywords:

Fluctuating environment

Phenotypic switching

Dynamic heterogeneity

Limited resource

Chemostat model

Nonlinear dynamics

ABSTRACT

Phenotypic variability in a microorganism population is thought to be advantageous in fluctuating environments, however much remains unknown about the precise conditions for this advantage to hold. In particular competition for a growth-limiting resource and the dynamics of that resource in the environment modify the tradeoff between different effects of variability. Here we investigate theoretically a model system for variable populations under competition for a flowing resource that governs growth (chemostat model) and changes with time. This environment generally induces density-dependent selection among competing sub-populations. We characterize quantitatively the transient dynamics in this system, and find that equilibration between total population density and environment can occur separately and with a distinct timescale from equilibration between competing sub-populations. We analyze quantitatively the two opposing effects of heterogeneity – transient response to change, and fitness at equilibrium – and find the optimal strategy in a fluctuating environment. We characterize the phase diagram of the system in term of its optimal strategy and find it to be strongly dependent on the typical timescale of the environment and weakly dependent on the internal parameters of the population.

© 2012 Elsevier Inc. All rights reserved.

0. Introduction

The connections between spatial and temporal variation of environments and the corresponding variation of organisms inhabiting them is a fundamental problem in biology. Beyond and in addition to specialized mechanisms that organisms use to cope with varying environments, it has been proposed many years ago that maintaining a component of phenotypic variability can be a good strategy if the environment is unpredictably changing (Cohen, 1966; Levins, 1968; Lenormand et al., 2008). Much research was performed in order to understand the adaptive value of different stochastic behaviors, both theoretically and empirically (Meyers and Bull, 2002). At the population level, this adaptive value is manifested when maintaining a random heterogeneity induces a higher long-term fitness than any homogeneous state of the population. This effect, known as bet hedging, has been extensively studied both theoretically and experimentally, but still remains under much debate (Meyers and Bull, 2002; Simons, 2011).

Early work on bet-hedging considered discrete generations, and studied models in which the stochastic process describing variable behavior was uncorrelated (e.g. “adaptive coin flipping”, Cooper and Kaplan, 1982). However, the effect of bet hedging

as a population strategy depends strongly on the dynamics and characteristic timescales of the variable phenotype, which is in turn related to the modes of heritability. Natural environments are variable in many dimensions and over multiple timescales; biological variation arises by multiple mechanisms at all levels of organization multiple timescales (Rando and Verstrepen, 2007).

The accumulating evidence on multiple timescales in genetic and epigenetic inheritance was suggested to be a substrate for timescale selection in phenotypic switching models (Lachmann and Jablonka, 1996). These authors showed that switching between phenotypes can be advantageous in a slowly varying environment, and furthermore that the optimal switching time is proportional to the typical timescale of the environment. This result was later shown to hold for a more general model of n phenotypes and m environments (Jablonka et al., 1995; Kussell et al., 2005). Others (Wolf et al., 2005) considered the yet more general case which includes imperfect cellular sensing mechanisms, and showed that heterogeneity can be selected by a time varying environment if the sensing mechanism is unreliable or slow. Moreover, even if it is not an optimal strategy in terms of growth rate, dynamic heterogeneity can decrease growth rate variance and thus the probability of extinction.

When analyzing dynamics and growth strategies of microbial populations it is important to take into account feedback from the environment. Typically microorganisms compete for common resources, deplete those resources and their abundance feeds back onto their growth. This can be described in models as a

* Correspondence to: Department of Chemical Engineering, Institute of Technology, Technion, Israel.

E-mail address: nbrenner@technion.ac.il (N. Brenner).

population-density-dependence of the dynamics (Mueller, 1997, although there can be other sources of density dependence such as spatial crowding). How exactly one should model density-dependent selection in population dynamics has been the topic of much research and debate (Asmussen and Feldman, 1977; Boyce, 1984). The above mentioned previous studies on bet hedging have assumed that growth rate difference is constant and therefore there was no density-dependent selection.

Our purpose in the present study is to extend the formulation of evolutionary bet hedging to include the effects of density dependence through the competitive depletion of a resource, using a simple model system based on the dynamics of a chemostat. In the chemostat, growth is limited by a resource (usually a nutrient component of the medium) and takes place under continuous flow. Cell density and resource concentration are tightly coupled: increase of the cell density depletes the resource, which in turn decreases the growth rate. Different cell states, or species, that proliferate in this system compete with one another for the limiting resource, generally by density-dependent selection. This is because the dependence of growth on resource generally causes the growth-rate difference to change in time through the dynamics of the resource. (An exception occurs if the two functions differ strictly by a constant.) For infinitely heritable states, asymptotically mutual exclusion occurs, with the more efficient state inhabiting the chemostat (Smith and Waltman, 1995); for a finite inheritance time, or a nonzero switching rate between states, states can coexist. The chemostat imposes on the problem a natural time scale, so that the population needs to keep up with the wash rate and cannot grow arbitrarily slowly. Thus cell states that are not fit enough do not survive in the competitive environments. These dynamic properties modify the tradeoff involved in bet-hedging: on one hand, there is less tolerance to the maintenance of species that are less fit; on the other hand, density-dependent effects can modify the efficiency of selection of a small subpopulation.

The chemostat is an experimental tool which enables to bring evolution into the lab for quantitative long-term investigation of fundamental questions in evolution and evolvability (Dunham et al., 2002; Stolovicki et al., 2006; Stern et al., 2007). It is also a device of technological importance. From the theoretical point of view it serves as a simple model for an environment with competition for a flowing resource such as a lake or pond. It incorporates density-dependent selection in a continuous growth model in a natural way and avoids complications and instabilities often met by discrete population models. Theoretical work on the chemostat has focused almost exclusively on asymptotic analysis; however, in the face of a fluctuating environment asymptotic states are not reached and it is important to understand also the transient dynamics. Therefore this work is composed of two stages: we first establish some general results about the transient dynamics of competing populations in a chemostat, including a quantitative description of dynamic trajectories and analytic estimates of the relevant time scales. Second, we utilize these results to analyze and assess heterogeneity strategies available for a microbial population in a changing environment in a chemostat.

1. Transient dynamics of takeover

The appearance of a species or sub-population better-fitted than the resident one generally causes it to become dominant. In a chemostat, where the environment induces selection by competition for resource and washout, this eventually results in mutual exclusion (Smith and Waltman, 1995). In this section we describe the transient dynamics of this process and provide quantitative estimates for its characteristic time scales. We show that equilibration between the two competing sub-population and

between populations and environment are separate processes that can occur on distinct time scales. For related recent results see Hajji and Rapaport (2009).

Imagine a population of density u , whose growth rate depends on a resource ζ through the nonlinear function $\mu_1(\zeta)$, is growing at steady state in the chemostat. A second species v with growth curve $\mu_2(\zeta)$ and with the same yield appears in small amounts within the environment. We assume that the number of invading cells, although very small relative to the equilibrium density, is large enough to ignore stochastic effects and drift (Gillespie, 2004; Desai and Fisher, 2007). The dimensionless equations governing the dynamics are

$$\begin{aligned} \frac{d\zeta}{dt} &= 1 - \zeta - \mu_1(\zeta)u - \mu_2(\zeta)v \\ \frac{du}{dt} &= (\mu_1(\zeta) - 1)u \\ \frac{dv}{dt} &= (\mu_2(\zeta) - 1)v \end{aligned} \quad (1)$$

with $\mu_1(\zeta)$ and $\mu_2(\zeta)$ general nonlinear monotone increasing functions. The fixed points for this system are the empty state $(\zeta^*, u^*, v^*) = (1, 0, 0)$, an unstable fixed point $(\mu_1^{-1}(1), 1 - \mu_1^{-1}(1), 0)$ corresponding to the subdominant species inhabiting the chemostat, and a stable fixed point $(\mu_2^{-1}(1), 0, 1 - \mu_2^{-1}(1))$ with only the dominant species (see Appendix B). Dominance in the chemostat is determined by the lowest value of $\mu^{-1}(1)$, the steady-state value of the limiting nutrient concentration. In general this is not necessarily the highest maximal growth rate. However, in what follows we shall assume a constant nutrient-independent selection coefficient s such that $\mu_2(\zeta) = s\mu_1(\zeta)$; in this case the dominant species is indeed the one with the highest maximal growth rate. It is noted that this relation between growth functions induces density-dependent selection between the two types, as does any other arbitrary choice of growth functions except for the special case of $\mu_2(\zeta) = s + \mu_1(\zeta)$.

While the asymptotic result of mutual exclusion is a well-known corollary of the above described fixed points, we are here particularly interested in the transient dynamics that lead to it. Fig. 1 illustrates the dynamics of takeover displayed as the trajectories over time (1a,1c) and in the (u, v) -phase plane (1b,1d), for two sets of parameters corresponding to small ($s = 1.08$; 1a,1b) and large ($s = 2$; 1c,1d) selection coefficients. The transient dynamics in both cases start with an invasion phase, where the invading population is still a small minority and has a negligible effect on the nutrient concentration in the environment and on the density of the resident population. After this initial phase the dynamics differ for the two sets of parameters. For small selection coefficient, Fig. 1(a) shows a second, takeover phase, in which the invading population takes over in terms of composition, and the environment adjusts itself accordingly on a similar time scale. The picture in the phase plane (u, v) , is illustrated in Fig. 1(b), where it is seen that the trajectory forms nearly a straight line. In contrast, Fig. 1(c), (d) show that for a large selection coefficient the dynamics is composed of three distinct phases. The first two are similar to those of Fig. 1(a): an initial invasion phase and a takeover phase in which all dynamic variables are changing simultaneously. However here the total population and environment decay quickly to their equilibrium values, and a third phase appears in which the population internal composition relaxes on a slower timescale. In the (u, v) , plane the two takeover phases are reflected by two different slopes. Phase III, the population equilibration phase, is characterized by a trajectory which is near the line $u + v = \text{const}$ (illustrated by a dashed line in the figure).

During the invasion phase, the population is composed almost entirely of the resident population and the environment is nearly

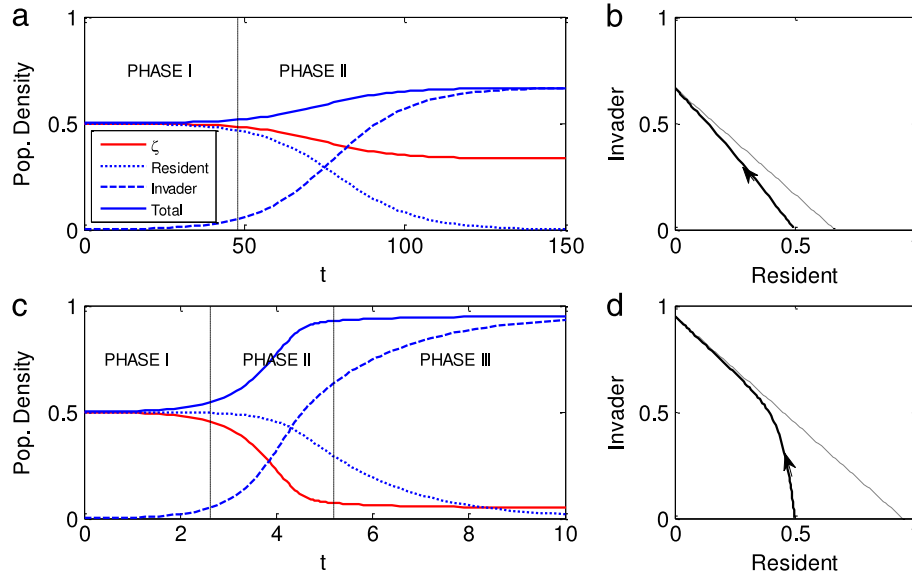


Fig. 1. Transient dynamics of takeover in the chemostat for small (a,b) and large (c,d) selection coefficient. In (a,c) the dynamical variables are plotted as a function of time: concentrations of resource (solid red line), resident species (dotted line), invading species (dashed line) and total population (solid blue line). In phase I the resource is still controlled by the resident population. At low selection coefficient (a), phase II is the takeover phase where all dynamical variables equilibrate on similar timescales. A large selection coefficient drives a rapid equilibration between the total population and the environment (c, phase II), and then a slower equilibration continues between the two competing species (phase III). In (b,d) the same trajectories are shown in the phase plane of the two species. (Parameters: Monod growth functions with $\alpha_1 = 1.2$, $\kappa = 0.1$; selection coefficient $s = 1.08$ or 2). (For interpretation of the references to colour in this figure legend, the reader is referred to the web version of this article.)

constant at ζ^* , and thus the invading population v approximately satisfies

$$\frac{dv}{dt} = (\mu_2(\zeta^*) - 1)v = (s - 1)v \quad (2)$$

and grows exponentially with a rate known as the invasion exponent (Diekmann, 2003): $v(t) \approx v_0 \exp\{[\mu_2(\zeta^*) - 1]t\}$, until reaching a threshold where it starts to affect the environment. Defining the end of the invasion phase by a threshold on the final fraction θ_i of the invading population relative to the resident one, we can estimate the invasion time as $v_0 \exp\{[\mu_2(\zeta^*) - 1]t\} = \theta_i(1 - \zeta^*)$, giving

$$t_{\text{inv}} = \frac{\ln \left[\frac{\theta_i}{v_0} (1 - \zeta^*) \right]}{\mu_2(\zeta^*) - 1} = \frac{\ln \left[\frac{\theta_i}{\theta_0} \right]}{s - 1} \quad (3)$$

where θ_0 is the initial fraction of the invading population. Thus the invasion time is inversely proportional to the difference in growth rate between the resident and invading populations at the initial environment (by definition the resident population has a growth rate of 1 at its steady state). In this part of the dynamics, since the change in and in total density is negligible, the result is identical to that of two populations with a fixed growth rate difference.

In the second phase of dynamics, the invading population is starting to detectably diminish the growth resource in the environment and this, in turn, affects the populations' growth rates. This can be viewed as a density-dependent selection where the frequency dynamics are governed by a time-varying growth rate difference. Although the dynamics of density and frequency are coupled they do not necessarily have the same characteristic time scale; observation of Fig. 1 shows that in the first case of small selection coefficient, the substitution of the resident by the invading species takes place at the same time as the environment adjusts itself to the new steady state value. By contrast, a large selection coefficient induces a separation between these times, as the environment equilibrates first and then competition and substitution takes place while the environment and total population are approximately at steady state.

The “frequency takeover time”, defined as the time it takes the invading population v to change from an initial small fraction θ_i to a final fraction $\theta_f = 1 - \theta_i$, is given by (Appendix B)

$$t_{\text{freq}} = \frac{s + 1}{s - 1} \ln \left(\frac{1 - \theta_i}{\theta_i} \right) - \ln \left(\frac{v^*}{u^*} \right), \quad (4)$$

where u^*, v^* are the equilibrium densities of the resident population before and after invasion. The main feature of this expression is that it decreases very slowly and is bounded from below with increasing selection coefficient s . Thus the final stage of the “selective sweep” is governed by the washout rate and not by the selection coefficient. This is shown in Fig. 2 (circles), and is contrasted with the takeover time in an open system (dashed line).

At large selection coefficient s , a considerable adjustment of the environment is required, and the transition from one fixed point to the other involves a large change in ζ^* . As seen in Fig. 1(c), (d), equilibration between the total mixed population and the environment takes place first, and then there is an internal process of substitution between the two cell types. Since the total population density is both an observable quantity and one that is associated with fitness (see below), it is of interest to estimate the typical time it takes the total population to reach its equilibrium value. In terms of Fig. 1 we are interested in estimating the time till the end of Phase II. Our estimate is based on the structure of the trajectories in phase space, which are composed of two parts associated with phases II and III of the dynamics; for details see Appendix B. The “density takeover time” is found as

$$t_{\text{dens}} \cong \frac{1}{s - 1} \left[-s \ln \left(1 - \frac{\Delta \zeta^*}{u^*} \beta \right) + \ln \left(1 - \frac{\Delta \zeta^*}{u^* \theta_i} (1 - \beta) \right) \right] \quad (5)$$

where $\beta = \eta_1/(1 - \eta_2)$ and η_1, η_2 are parameters determining the eigenvalues of the Jacobian matrix at the unstable fixed point. This estimate is shown in Fig. 2 (squares) together with the numerical calculation of the takeover time (corresponding solid line). The expression inside square brackets is weakly dependent

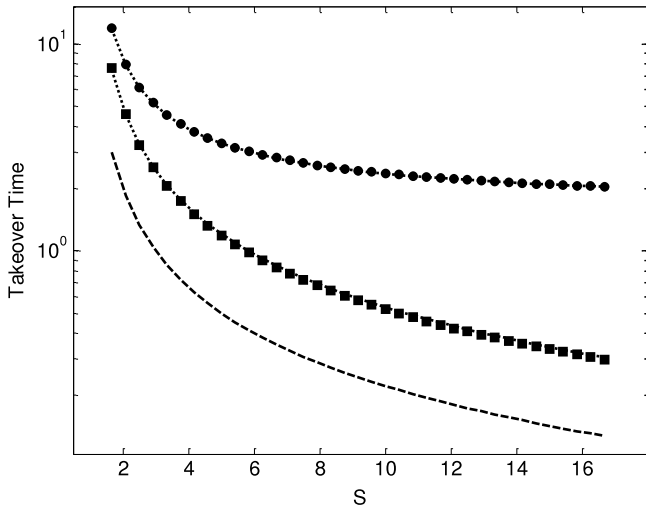


Fig. 2. Takeover timescales in the two species problem. An invader population with selection coefficient s starts from an initial small relative concentration θ_i . Two characteristic timescales of the transient dynamics are plotted: frequency takeover time – the time for the invader population to reach a threshold relative concentration θ_f (exact expression in chemostat – circles, numerical solution – corresponding dotted line), and density takeover time – the time for the total population, resident + invader, to reach θ_f of its equilibrium value (computed by eigenvector method – squares, numerical solution – corresponding line, see Appendix B). For comparison, the takeover time for an open system with no limited resource, defined by relative concentrations, is shown (dashed line). $\theta_i = 0.01$, $\theta_f = 0.9$.

on s and therefore the dependence of the takeover time can be approximated as $c/(s - 1)$, where c is a constant. This time has a functional form similar to the invasion time or the takeover time (which are the same) in an open system (see Fig. 2).

In summary, the two-species dynamics in a chemostat can be characterized by two timescales characterizing the frequency and density dynamics, which can be distinct despite the coupling between them. While the first is limited from below by the typical chemostat time, the second decreases rapidly with selection coefficient. Thus for large s , although the frequency takeover time decreases, it does so very slowly and a much more dramatic effect is found in terms of the density takeover time. The total population reaches equilibrium with the environment first, and then the different sub-populations equilibrate to obtain the equilibrium population composition. In the parameter range presented in Fig. 2 the two timescale can differ by almost an order of magnitude. This two-stage transient dynamics can be significant from the point of view of population survival and fitness: following a change in environment the total population may establish its stability very rapidly thanks to the existing variability, although the more fit species will take longer than this to actually take over the population in terms of its composition.

2. Phenotypic switching in the chemostat

Phenotypic traits that affect microorganism growth are not perfectly inherited, and can have correlation times ranging from less than a generation to several generations (Lord and Wheals, 1980; Sigal et al., 2006). In preparation for our main goal of investigating the dynamic heterogeneity of a chemostat with a varying environment, we present here for completeness the main results for a chemostat in a constant environment but with finite transitions between two states. These transitions ensure that heterogeneity remains and is not lost by selection.

We model the finite stability of the cellular states by first-order transitions between them, with rates γ_1 , γ_2 :

$$\begin{aligned} \frac{d\zeta}{dt} &= 1 - \zeta - \mu(\zeta)u - s\mu(\zeta)v \\ \frac{du}{dt} &= (\mu(\zeta) - 1)u - \gamma_1u + \gamma_2v \\ \frac{dv}{dt} &= (s\mu(\zeta) - 1)v + \gamma_1u - \gamma_2v. \end{aligned} \quad (6)$$

The dynamical system (6) with nonzero γ_1 , γ_2 admits only one nontrivial fixed point which is a coexistence state. As the transition rates decrease to zero the system goes through a bifurcation, the coexistence states disappears and a pair of fixed points, one stable and one unstable, emerge; this is mutual exclusion. For small transition rates, the structure of phase space is affected by the vicinity of the bifurcation point, the ghost of the unstable fixed point distorts the trajectories and they spend a long time near it (see Appendix C).

The coexistence fixed point for the system with nonzero transition rates can be characterized by the ratio of concentrations $p(s, \gamma_1, \gamma_2) = u^*/v^*$ (see Appendix C). The fraction of the fitter state in the total population is expressed as $f = 1/(p + 1)$, whereas the fixed point value of the resource, ζ^* , satisfies the following implicit equation

$$\mu(\zeta^*) \frac{p}{p + 1} + s\mu(\zeta^*) \frac{1}{p + 1} = \mu(\zeta^*) \frac{p + s}{p + 1} = 1. \quad (7)$$

This equation defines an equilibrium growth curve $\tilde{s}\mu(\zeta)$ for the total population, such that $\zeta^* = \mu^{-1}(1/\tilde{s})$, where $\tilde{s} \equiv (p + s)/(p + 1)$. For a Monod growth function, $\mu(\zeta) = \frac{\alpha\zeta}{\zeta + \kappa}$, the limiting resource and population concentrations at steady state as a function of the ratio p can be found explicitly:

$$\zeta^* = \frac{\kappa}{\tilde{s}\alpha - 1}. \quad (8)$$

It is of interest to compare the fixed point of this dynamically heterogeneous population to that of a freely growing population with constant growth rates. Here a fixed point is not reached but the fractions attain a limiting value. Denoting the free growth rates by μ and $s\mu$ and the switching rates as before by γ_1 , γ_2 , we compare the limiting fraction f at small transition rates and as a function of selection coefficient. For the open system the fraction can be approximated as

$$f \approx 1 - \frac{\gamma_2}{\mu(s - 1)}, \quad (9)$$

whereas in the chemostat we find

$$f \approx 1 - \frac{s\gamma_1}{s(1 + \gamma_2 + \gamma_1) - (1 + \gamma_1)}. \quad (10)$$

It is seen that for large selection coefficient the fraction of favored cells approaches unity in the open system while in the chemostat it is bounded by a function of the transition rates, as illustrated in Fig. 3. This can be understood by the fact that near equilibrium the favored type has a selective advantage of $1 - 1/s$, whereas in an open system this advantage is always proportional to $(s - 1)$.

3. Fluctuating environments

We now combine the results of previous sections to address the main point of this paper: phenotypically switching organisms in a fluctuating environment chemostat. We consider an environment which switches between two possible states E_1 and E_2 , forming a sequence, either periodic or random in time. The cells in the population have two possible cell states, each better fitted to one type of environment and suffering a decrease in growth in the other environment. In the simplest case there is symmetry between the two states in the two environments. This model was

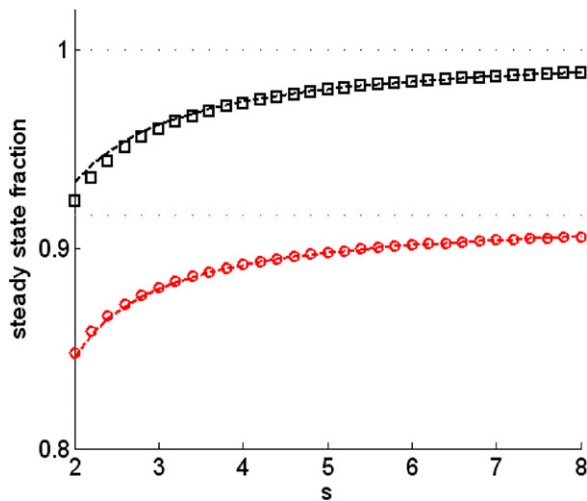


Fig. 3. Fraction of faster-growing cells in a population at equilibrium with symmetric transitions between the two types. In an open system with unlimited resource (squares), this fraction approaches unity for large s . Competition for resource limits this fraction: in a chemostat (circles), it approaches a maximal fraction smaller than one that depends on the transition rates. Parameters: $\mu = 1.2$, $\kappa = 0.1$, $\gamma_1 = \gamma_2 = 0.1$. Symbols denote numerical computation while dashed lines are the approximations given in the text.

studied in previous work on unlimited environments (Lachmann and Jablonka, 1996; Thattai and Oudenaarden, 2004; Kussell and Leibler, 2005; Donaldson-Matasci et al., 2008). The model of Eq. (6) describes similarly a two-state system with competition for a limited resource, if it is understood that once the environment changes state the roles of the two states are switched. To analyze the population dynamics we must now address the subtle issue of defining fitness of the population.

For populations in an open unlimited environment, fitness is usually defined by the mean growth rate in the population. If f denotes the fraction of cells in the faster growing state, with specific growth rate μ_2 , then this mean growth rate is $f\mu_2 + (1 - f)\mu_1$. This is a monotonic function of the fraction f , and therefore maximizing fitness is here equivalent to maximizing f . In a chemostat the situation is quite different: at equilibrium the net growth rate is determined externally by the washout rate. In transient states, instantaneous growth rate is tightly coupled to the instantaneous concentration of limiting nutrient in the system. The question of what microorganism metabolism is optimized for (if at all) is a nontrivial question (Schuetz et al., 2007). Under conditions of nutrient limitation, it has been suggested that metabolism is optimized for quantities related to total biomass production. This means viewing the total biomass as an indicator of fitness, and under varying conditions—the biomass averaged over time. Considering also that in a finite population a small amount of biomass increases the probability of extinction, it is further reasonable to adopt this measure of fitness, as we do in what follows.

Among the strategies available to the population in the face of a changing environment, there are those that involve sensing the environment and those that do not (Wolf et al., 2005). We consider first the case where there is no sensing mechanism, and ask under what conditions blind bet-hedging, or “coin flipping” (Cooper and Kaplan, 1982), can increase fitness. Then we consider a response to the environment that incurs a delay time and ask whether a biased bet-hedging can improve on a delayed response mechanism.

No sensing: pure strategy vs. random transitions.

If the cells do not have any sensing mechanism, the transition rates are independent of the environment and for simplicity can be assumed the same in both directions ($\gamma_1 = \gamma_2 = \gamma$ in Eq. (6)).

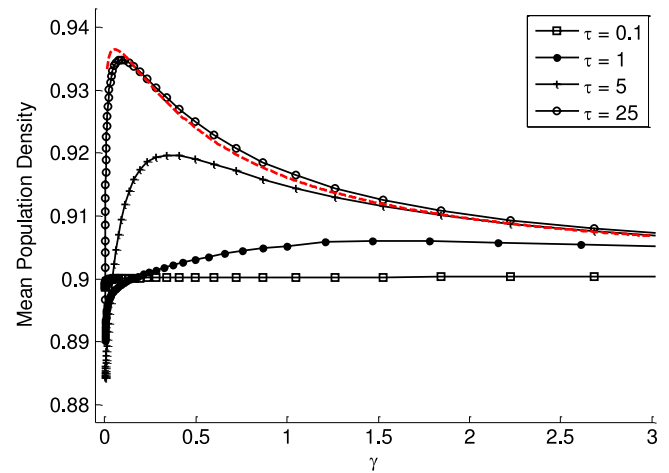


Fig. 4. Population fitness with random switching (equal transitions between the two states). Population fitness – time-averaged density – is plotted as a function of transition rate γ in a periodically changing environment with period τ . For environments that change slowly enough an optimal value for the random transition rate emerges. The approximation described in the text, taking into account the tradeoff between steady-state mixture effects and transient recovery, is shown as a dashed red line. Parameters: $\alpha_1 = 1.2$, $\kappa = 0.1$, $s = 2$. (For interpretation of the references to colour in this figure legend, the reader is referred to the web version of this article.)

The pure strategy, where cells remain in the same state at all environments despite loss of fitness in some of them, is obtained as the limit $\gamma_1 = \gamma_2 = 0$. Under what conditions is it better for the population to have a nonzero transition rate between the two states, even though these transitions are completely random? Fig. 4 shows the population fitness in a periodic environment with random transitions between two states, computed by numerically solving the Eqs. (6) with a periodically changing environment with different periods τ . The fitness is plotted as a function of the transition rate γ , and it is seen that if the environment changes slowly enough there exists an optimal nonzero transition rate which induces a maximal fitness.

Using the results of the previous sections, for a slowly changing environment we can qualitatively analyze the tradeoff which leads to the nonzero optimal transition rate. The assumption of slow variation implies that in each environment the system is allowed to relax close to its equilibrium. After this relaxation, transitions cause a mixture of the two states and thus fitness decreases; this effect becomes more severe as the transition rate increases due to a larger equilibrium ratio p of disfavored cells. On the other hand, once the environment changes, the same near-equilibrium fraction of previously disfavored individuals will take over and adjust the population to the new situation. Here fitness will increase with γ since the initial condition for the takeover dynamics will be more favorable at large γ . It is clear from these considerations that the optimal solution will depend on the frequency of environment changes relative to the times of transient dynamics. Fig. 5 shows for illustration some typical trajectories in a periodic environment with $\tau = 10$ and different values of transition rates.

These arguments show that $p(\gamma, s)$, the ratio between cell types at equilibrium, is a key factor affecting the tradeoff. We use it to quantify the mean fitness over many periods of the environment and to predict the optimal transition rates. For a Monod growth function, the total biomass at equilibrium is

$$u + v = 1 - \zeta^* = 1 - \frac{\kappa}{\tilde{s}(\gamma, \alpha) - 1}, \tag{11}$$

where we recall that $\tilde{s} = (p(\gamma) + s)/(p(\gamma) + 1)$. This contribution to fitness, a slowly decreasing function of γ , will be significant for high transition rates. It will have a stronger effect for slower

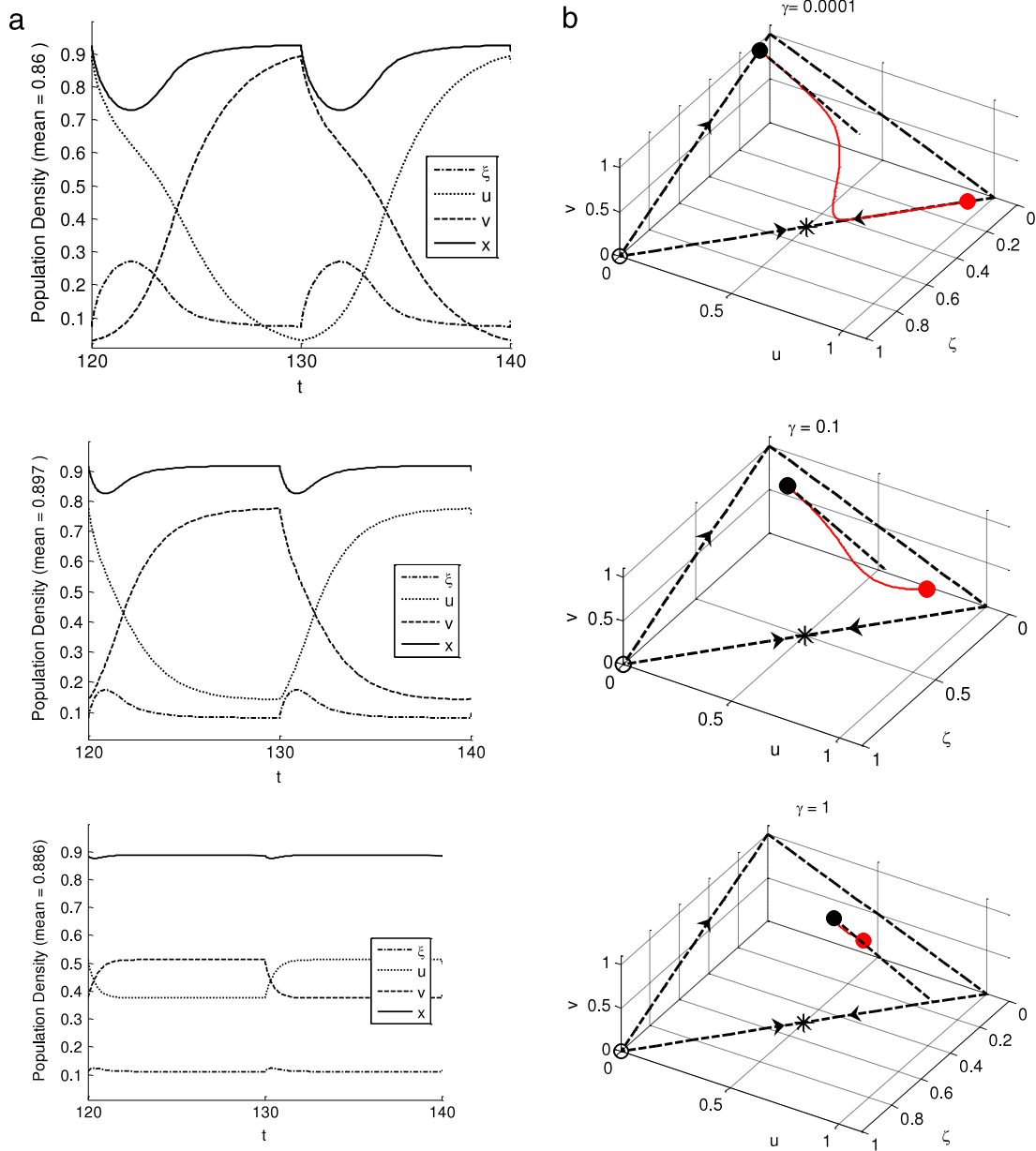


Fig. 5. Dynamics in a time-periodic environment with different transition rates among states. The environment switches between two states every 10 time units. Trajectories are shown for two periods after a long time such that a time-varying steady state has been reached (left column), and corresponding trajectories following environment change are traced in phase-space (right column). (Top) Very small transition rates $\gamma = 10^{-4}$. At the end of a stretch of constant environment, the sub-optimal sub-population decreases to a very low concentration; see for example the dashed line (v) at $t = 120$. This is reflected in phase space by a coexistence fixed point very close to the boundary where $v = 0$ (red dot in right column). After a long time in this environment the trajectory comes near this coexistence point. Upon environment change, the characteristics of the two states are interchanged and the new coexistence fixed point is close to the other boundary $u = 0$ (black dot). The red dot is now the initial condition for convergence to the black dot. The proximity of this initial condition to the boundary and thus to the stable direction of the “ghost” unstable fixed point corresponding to $\gamma = 0$, forces the trajectory to move through large ζ regions of the plane. Since the plane $u + v + \zeta = 1$ is invariant under the dynamics, this portion of the trajectory causes a fitness decrease. (Middle and Bottom) As γ increases, the coexistence fixed points move away from the boundaries and the trajectories flow between the old and new fixed points more smoothly; the effect of the ghost unstable fixed point disappears. Parameters: $\mu = 1.2, \kappa = 0.1, s = 2$. (For interpretation of the references to colour in this figure legend, the reader is referred to the web version of this article.)

environments where a larger fraction of the time is spent near equilibrium.

The other side of the tradeoff, the loss of fitness due to transient dynamics upon environment change, is most important for small transition rates. In this region it is primarily determined by the initial conditions of the previous equilibrium and by the selection coefficient s ; the takeover time to reach the new steady state can be approximated as (Appendix C)

$$t_{tk} \cong -\frac{(s+1)}{(s-1)} \ln p. \tag{12}$$

Now suppose that the environment is changing periodically, spending a time τ in each state. In a symmetric model, where the two states exchange role in the two environments, the average biomass in a period is approximately

$$\begin{aligned} \langle f \rangle &\approx \frac{\tau - t_{tk}}{\tau} (1 - \zeta^*) + \frac{t_{tk}}{\tau} \varepsilon (1 - \zeta^*) \\ &= (1 - \zeta^*) \left[1 + \frac{t_{tk}}{\tau} (\varepsilon - 1) \right], \end{aligned} \tag{13}$$

where ε is an effective parameter measuring the average fitness

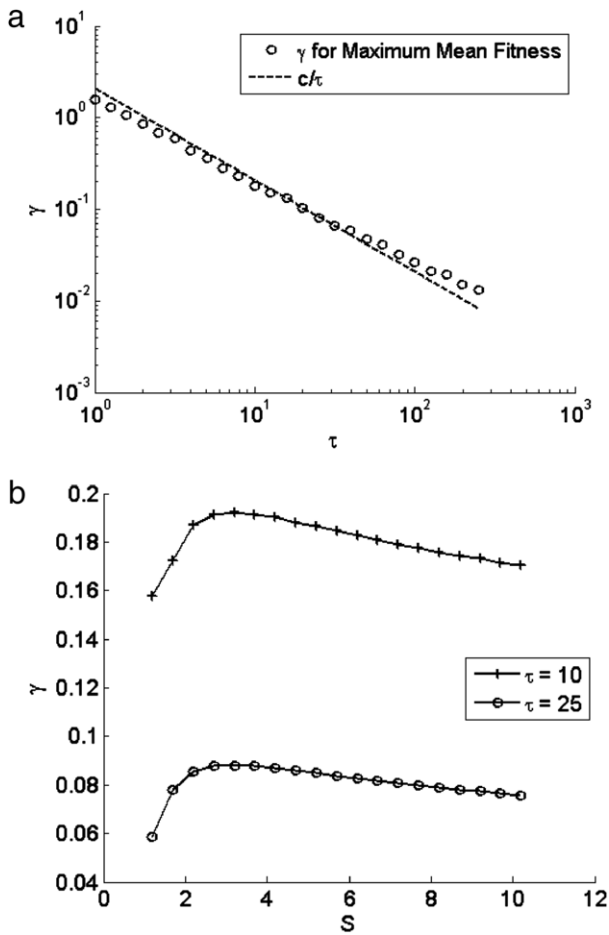


Fig. 6. Symmetric transition rates that maximize mean population fitness in a periodic environment. The optimal transition rate depends weakly on s , but strongly and approximately inversely on environmental period.

during the transient period. This expresses the fitness as a product of two terms, both of which depend on γ through p : the first is the equilibrium fitness and the second describes the transient. In terms of the ratio p , the equilibrium population density $(1 - \zeta^*)$ decreases slowly whereas the second one increases rapidly, as $(-)$ the logarithm of the equilibrium ratio

$$\langle f \rangle \approx \left[1 - \frac{\kappa}{\left(\frac{p+s}{p+1}\right)\alpha - 1} \right] \left[1 + \frac{(1-\varepsilon)s+1}{\tau} \frac{1}{s-1} \ln p \right]. \quad (14)$$

This approximation is depicted by a dashed line in Fig. 4 for the slowest environment. It is seen that the two contributing factors – one decreasing and one increasing as a function of γ – give the quantitative description of the tradeoff of bet-hedging in our model.

The calculated optimal transition rate depends most strongly on the environment period τ , and weakly on the selection coefficient s . This is illustrated in Fig. 6. The dependence on τ is approximately inverse, similar to results found for an open system (Lachmann and Jablonka, 1996; Kussell and Leibler, 2005). All the results presented in Figs. 4–6 are found to hold also for an environment which changes randomly between its two states, according to a Poisson process with a rate $1/\tau$.

As discussed above, the definition of fitness that we have used to formulate the optimization problem for the population dynamics is somewhat arbitrary. In general other properties of the population can affect its survival, for example the minimum number of cells

strongly affects the probability of extinction. We have seen in Fig. 5 that the population density reaches its minimum shortly following the environment switch due to the abrupt change in state of the dominant resident population. How would this result change if we allowed the environment a gradual change of its state, as is more realistically the case in nature?

To answer this, we modified the model described by Eq. (6) to include a smooth change in environment rather than a step-function change. The time scale of this smooth change, τ_{sm} , is taken to be slightly shorter or similar to the environment switching timescale. The transient dynamics following such an environment change are depicted in Fig. 7 for three values of τ_{sm} . The effect on the population trajectory is significant in terms of the minimal density reached; it becomes filtered for longer internal transition timescale, as can be expected. In terms of phase space trajectories, the ghost fixed point no longer has such a strong effect, because the dominant population does not become immediately unfit but rather both sub-populations have intermediate properties.

Using this modified model and computing again the time-averaged population density does not change the picture presented in Fig. 4 (data not shown): the minimal density increases but the transient takes longer to recover. Thus in terms of the long-term fitness defined above, there is little sensitivity to the gradualness of the environment change. However this result shows that the internal population structure can change dramatically while the total population density remains almost constant. This property can buffer the population over times where its internal structure is being modified to account for external changes, and decrease the amount of time where it suffers an extremely low density and is subject to high extinction probability.

Environment-dependent transition rates.

If cells can sense the environment, they can in principle induce a transition towards the more fit state in each given environment. The extreme limit of this situation is when each environment immediately defines all cells to be in the more fit state. More generally even if there is sensing that can bias the transitions in this way there remains a delay in the transition itself, that is most simply modeled by first order kinetics with different forward and backward transition rates. At the level of the population, this is described by the model of Eq. (6) with $\gamma_1 > \gamma_2$.

It is quite obvious that if the population can set the forward transition (from the unfit to the fit state) to be high enough, this will increase fitness. However, somewhat less intuitively, for a given forward transition rate, setting the backward rate nonzero can sometimes enhance fitness (Thattai and Oudenaarden, 2004). Stating this in different words, given that the induced transition has a speed limitation, an additional factor of dynamic heterogeneity can enhance fitness. To test whether this phenomenon occurs also in our model, we computed numerically the population fitness for a given forward transition rate as a function of the backward rate, see Fig. 8. It is seen that for a slow enough environment indeed there is a maximal fitness at a nonzero value of γ_2 . The fitness as a function of both transition rates is shown in Fig. 9; this plot shows similar characteristics for both periodic and random environment time sequences. Indeed, if the forward transition rate is high enough the optimal value of the backwards transition rate is zero (top left corner of the square). However for smaller values, there is a clear nonzero value of backward rate which optimized the fitness, and this value of almost constant before it decreases rapidly to zero. Thus the optimal value of the back-transition rate is weakly dependent on the forward transition rate. This plot can therefore be characterized by the crossover value of the forward transition rate for which dynamic heterogeneity can provide additional fitness to the population, the critical γ_1 . The dependence of this critical γ_1 on other system parameters (s, τ), is summarized in Fig. 10.

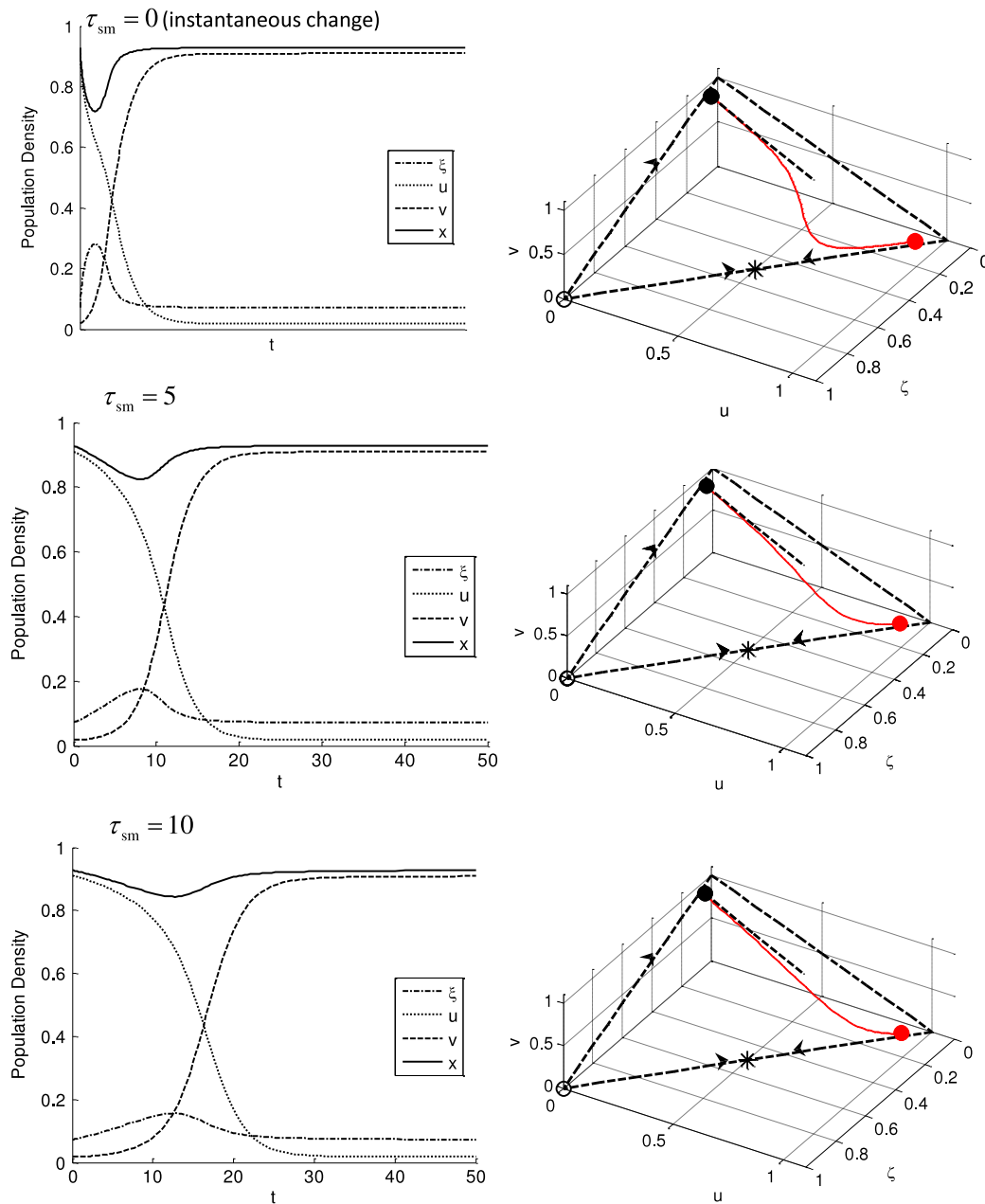


Fig. 7. Slower changes in cell state induce milder fluctuations in total population. The model presented in Eq. (6) was modified to include a gradual change of environment with a typical timescale τ_{sm} . The transient dynamics following an environment change at $t = 0$ is depicted in the left column and the corresponding phase space trajectories on the right column. It is seen that as the environment change of state becomes more gradual, the trajectory remains closer to the line $u + v = \text{constant}$. The population density time-averaged over the entire transient remains practically unchanged (not shown). Parameters: $\mu = 1.2$, $\kappa = 0.1$, $s = 2$, $\gamma = 10^{-3}$.

4. Summary and discussion

The idea of bet hedging as an adaptive population property that enhances fitness and survival in a fluctuating environment has been studied for many years (Meyers and Bull, 2002; Veening et al., 2008; Simons, 2011). Here these ideas were investigated in the context of a dynamic model with competition for limited resource, the chemostat model. The dynamics of the environment and the two-way interaction between the population and its growth-limiting resource induce a density-dependent component to the problem which can in principle modify the tradeoff involved in bet-hedging. While density-dependence has been introduced in many population models, much debate has taken place concerning the correct functional form of this dependence and its effect on population stability and evolutionary outcome (Asmussen and

Feldman, 1977). In this respect the chemostat model provides a natural, continuous way to describe density-dependence, which is induced simply from the consumption of resource under flow in the environment and from the difference in growth functions. The chemostat as a dynamical system has been the subject of much research, but this had focused almost exclusively on long-term asymptotics and not on transient dynamics. Recently it was found that if the difference in properties of the competing species is small, the timescale to reach mutual exclusion can be exceedingly long (Hajji and Rapaport, 2009). When the environment is changing it is important to understand the transient dynamics under general conditions.

We have characterized the transient dynamics of takeover among competing species in terms of two separate time scales of takeover: the frequency takeover time, defined by the time it

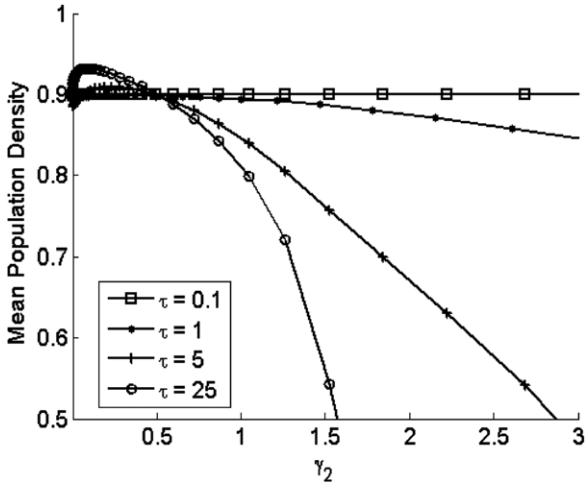


Fig. 8. Mean population density with fixed forward (towards the more fit state) transition rate as a function of back transition rate for different environment periods ($s = 2, \kappa = 0.1, \gamma_1 = 10^{-3}$). For very short environment periods (squares), the mean fitness is almost independent of back transition. As environment period increases, an optimal back transition rate emerges.

takes the invading species to become a considerable fraction of the population, and the density takeover time, defined by the time it takes the total population density to become a considerable fraction of its equilibrium value. We have shown that these times are generally distinct; in the limit of large selection coefficient

the latter is significantly shorter. The structure of the phase plane trajectories was characterized and used to obtain approximations for these time scales. This separation of timescales between internal dynamics and total population dynamics has been recently observed in a related model (Elhanati et al., 2011). The general conditions under which it holds and its implication on population survival are subjects for future research.

Bet-hedging can be realized by allowing transitions between different cell states, and thus maintaining a variable population structure even in a constant environment. With such transitions the fixed-point of mutual exclusion is replaced by a fixed-point of coexistence. For two competing sub-populations u, v . This fixed point resides in the interior of the manifold $u + v + \zeta = 1$. We have found that the fraction of the sub-optimal sub-population in this fixed point approaches a finite limit even for very large selection coefficient, in contrast to a system without competition where this fraction approaches zero.

In a fluctuating environment, these characteristics enable us to assess enabled us to assess the advantage of dynamic heterogeneity, where two states are available to the cells with a finite rate of transition between them. The tradeoff between a decrease in the steady-state fitness due to the presence of a nonzero fraction of unfit cells, and the speed of takeover of this minority as the environment changes, was calculated. We found that for a slowly varying environment there is a nonzero value of transition rate among the cell states which maximizes the mean cell density over time. This optimal value was found to depend strongly on the typical time scale of the environment and weakly

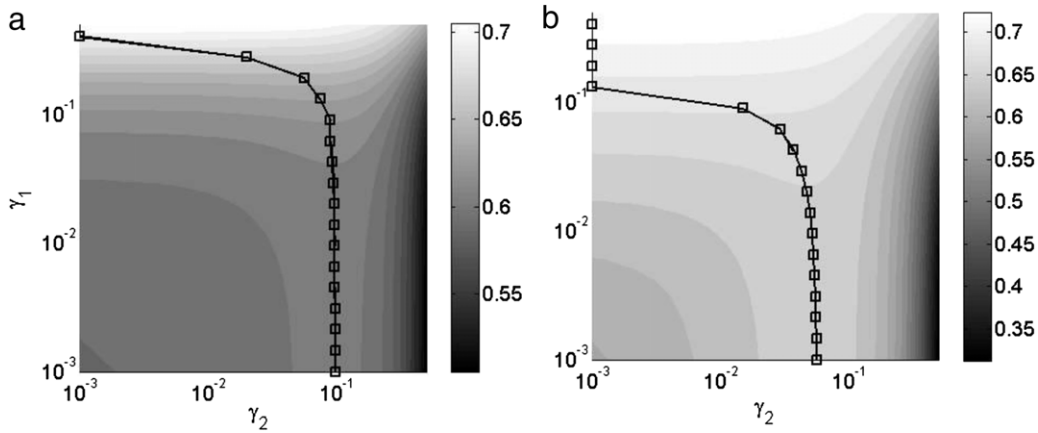


Fig. 9. Grayscale plots of the mean population fitness in changing environments for different phenotypic transition rates. Left: periodically changing environment, Right: environment changing according to a Poisson process with mean time τ . $\tau = 5, s = 2, \alpha = 1.2, \kappa = 0.1$. When γ_1 is large (top left hand corner), it is best to have a zero γ_2 . For low γ_1 , there is a ridge of γ_2 values where mean fitness is at a maximum. Its value is weakly dependent on γ_1 .

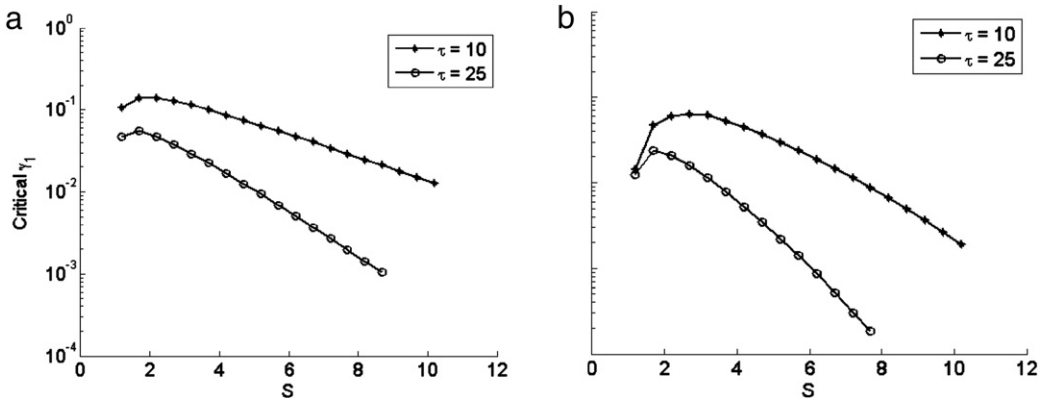


Fig. 10. Critical transition rates for different system parameters. For each value of s and τ this figure shows the critical value of γ_1 for which there exists an advantage for dynamic heterogeneity. This value corresponds to the “knee” in Fig. 9. (a) Periodic environment with time τ . (b) Poisson process of environments with mean duration τ .

on internal system parameters, such as the selection coefficient and the induced transition rate. The main contribution to the transient decrease in fitness in this model comes about from the sudden change of environment and cell state of the dominant sub-populations since it “controls” the environment and the change causes a sharp decrease in total cell density. When changes in the environment are more gradual, the control of the environmental resource remains robust against these changes. Although the long-term time-averaged population density is not significantly changed, its temporal modulations are less abrupt and thus the population is less prone to extinction. Another implication of this observation is that the total biomass can be stable or change only slightly, but the internal population structure and composition can at the same time undergo dramatic modulations (see Fig. 7).

Appendix A. Single species in the chemostat

The problem of a single species growing in a chemostat is classic and well known. We present here for completeness a general formulation in terms of linear stability analysis, showing how all properties of the phase plane of the dimensionless problem are determined by local parameters of the growth function with a simple geometric interpretation.

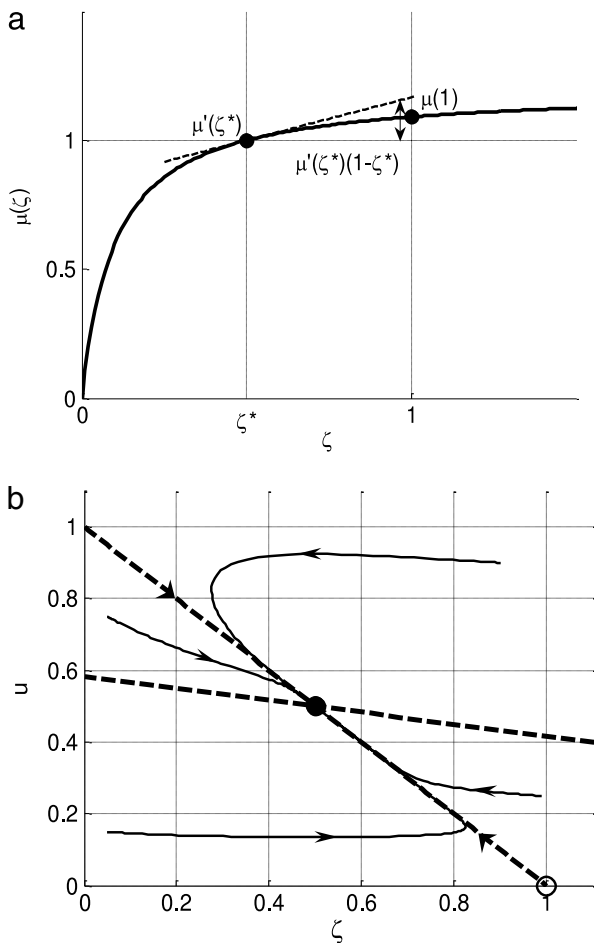


Fig. A.1. (a) Geometric interpretation of the parameters governing the chemostat phase plane. These parameters were calculated by using linear stability analysis and contain all the information regarding the dynamics of the system around its fixed points. (b) Phase plane of the single species chemostat model with Monod uptake growth function ($\alpha = 1.2, \kappa = 0.1$). The stable fixed point is at $\{0.5, 0.5\}$ and the unstable fixed point is at $\{1, 0\}$. The dashed lines denote the eigenvectors corresponding to the nontrivial fixed point.

If the chemostat is inhabited by a single species with a growth rate function $\mu(\zeta)$, the dimensionless equations of motion are

$$\begin{aligned} \frac{d\zeta}{dt} &= 1 - \zeta - \mu(\zeta)u \\ \frac{du}{dt} &= (\mu(\zeta) - 1)u. \end{aligned} \tag{A.1}$$

In these units the typical time of the chemostat (dilution time) is 1, and the concentration of limiting nutrient in the feed is also 1. This system has two fixed points $(\zeta^*, u^*) = (1, 0)$ and $(\mu^{-1}(1), 1 - \mu^{-1}(1))$. The Jacobian matrix is given by

$$J = \begin{pmatrix} -1 - \mu'(\zeta)u & -\mu(\zeta) \\ \mu'(\zeta)u & \mu(\zeta) - 1 \end{pmatrix}$$

where $\mu'(\zeta)$ denotes the derivative. At the trivial fixed the two eigenvalues are $\{-1\}$ and $\{\mu(1) - 1\}$ with eigenvectors $(1, 0)$ and $(-1, 1)$ respectively. The parameter $\mu(1)$ controls the bifurcation of this fixed point, as it loses its stability when $\mu(1) > 1$; it also determines the direction of the corresponding eigenvector. At the nontrivial fixed point $\mu(\zeta) = 1$, and the eigenvalues are $\{-1\}$ and $\{-\mu'(\zeta^*)u^*\}$ with corresponding eigenvectors $(1, -\mu'(\zeta^*)u^*)$ and $(-1, 1)$. Once again both the stability of the fixed point and the direction of one of the eigenvectors is determined by a single parameter, $\eta = \mu'(\zeta^*)u^* = \mu'(\zeta^*)(1 - \zeta^*)$; this is the product of the slope of the growth function and the population concentration at the fixed point (see Fig. A.1(a)). The phase space flow (Fig. A.1(b)) is determined by this same parameter, with a crossover value of $\eta = 1$ in which the two eigenvalues become degenerate. We shall assume that they are not degenerate. The line connecting the two fixed points, $\zeta + u = 1$, is an invariant manifold of the system (Smith and Waltman, 1995).

Appendix B. Two competing species: the road to mutual exclusion

We here analyze the linear stability of the three dimensional system, with two competing species characterized by growth functions μ_1 and μ_2 :

$$\begin{aligned} \frac{d\zeta}{dt} &= 1 - \zeta - \mu_1(\zeta)u - \mu_2(\zeta)v \\ \frac{du}{dt} &= (\mu_1(\zeta) - 1)u \\ \frac{dv}{dt} &= (\mu_2(\zeta) - 1)v. \end{aligned} \tag{B.1}$$

This system obeys the principle of mutual exclusion, and accordingly its fixed points are $(1, 0, 0)$, $(\mu_1^{-1}(1), 1 - \mu_1^{-1}(1), 0)$ and $(\mu_2^{-1}(1), 0, 1 - \mu_2^{-1}(1))$. The structure in three-dimensional phase space is simplified by the fact that the dynamics in the planes $u = 0$ and $v = 0$ is identical to that of the single-species problem. Because of mutual exclusion, all three fixed points lie on the sides of the linear sub-space $(\zeta \geq 0, u \geq 0, v \geq 0)$. All 9 eigenvectors lie on the faces of the polygon defined by the union of these sides with the plane $\zeta + u + v = 1$. See Fig. B.1 for illustration.

More specifically, we can write the general form of the Jacobian matrix

$$J = \begin{pmatrix} -1 - \mu'_1(\zeta)u - \mu'_2(\zeta)v & -\mu_1(\zeta) & -\mu_2(\zeta) \\ \mu'_1(\zeta)u & \mu_1(\zeta) - 1 & 0 \\ \mu'_2(\zeta)v & 0 & \mu_2(\zeta) - 1 \end{pmatrix} \tag{B.2}$$

and examine its spectrum at the three fixed points of the system. At the trivial state $(1, 0, 0)$, the matrix takes the simple form

$$J = \begin{pmatrix} -1 & -\mu_1(1) & -\mu_2(1) \\ 0 & \mu_1(1) - 1 & 0 \\ 0 & 0 & \mu_2(1) - 1 \end{pmatrix}. \tag{B.3}$$

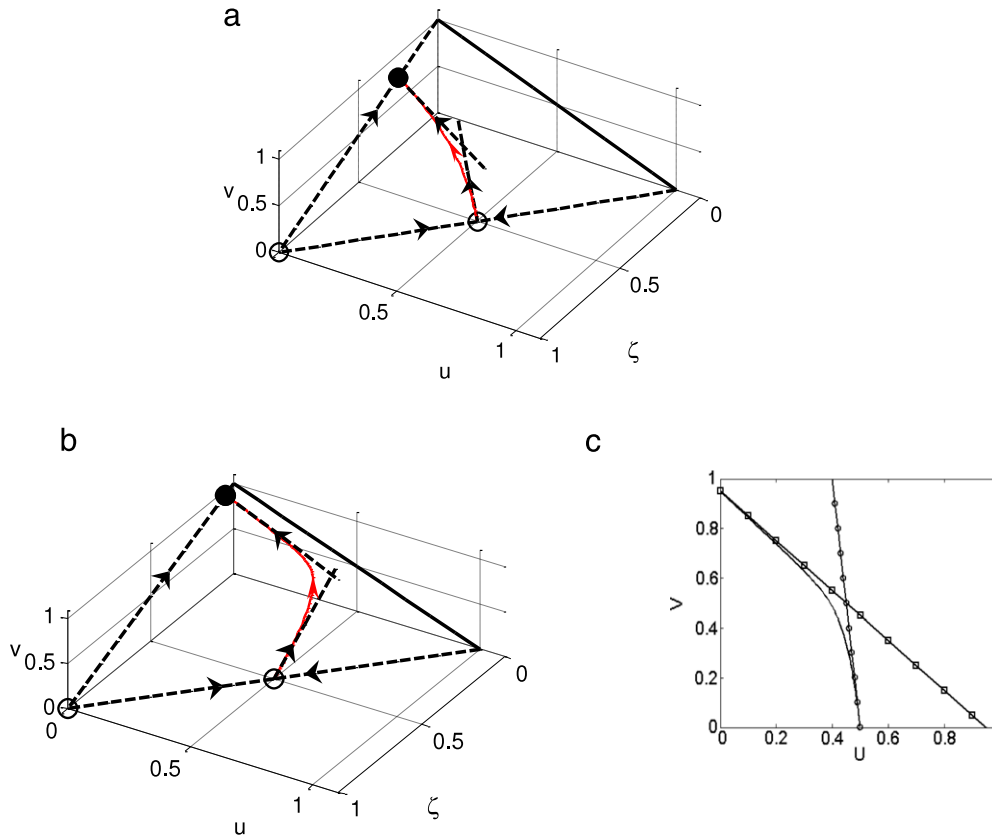


Fig. B.1. Phase space of the two species chemostat model with Monod growth curves ($\alpha_1 = 1.2, \kappa = 0.1$) and constant selection coefficient s . Dashed lines with arrows denote eigenvectors. (a) $s = 1.08$, (b) $s = 2$. (c) Projection of trajectory on the (u, v) plane for $s = 2$ and illustration of approximation. For large s , the takeover trajectory is approximately composed of two linear segments (see also Fig. 1(d)). The larger s , the better this approximation becomes. We estimate the takeover time for equilibration of the total population with environment by advancing along the eigenvector that leaves the unstable fixed point to the point of intersection of the two linear segments.

It has an eigenvalue $\{-1\}$ with eigenvector $(1, 0, 0)$ corresponding to no population in the chemostat; an eigenvalue $\{\mu_1(1) - 1\}$ with the eigenvector $(-1, 1, 0)$ in the (ζ, u) -plane, corresponding to only u -type population, and the same phase-plane structure as the single-species problem; and analogously the eigenvalue $\{\mu_2(1) - 1\}$ corresponding to a single-species problem in the (ζ, v) -plane. The third eigenvalue for the nontrivial fixed points is positive for one of them – rendering it unstable, and negative for the other – rendering it the only stable fixed point of the system. Suppose without loss of generality that v is dominant over u , then the third eigenvalue for the unstable point is $(1 - \eta_2, -\eta_1, \eta_1 + \eta_2 - 1)$ with $\eta_1 = \mu'_1(\zeta^*)u^*$ and $\eta_2 = \mu_2(\zeta^*)$; and for the stable point it is $(1 - \eta_4, -\eta_3, \eta_3 + \eta_4 - 1)$ with $\eta_3 = \mu'_2(\zeta^*)v^*$ and $\eta_4 = \mu_1(\zeta^*)$. In each case the star $(*)$ denotes values at the corresponding fixed point. This form of the eigenvalues shows manifestly that they are on the diagonal face of the 3-simplex as illustrated in Fig. B.1.

The first two parts in Fig. B.1 show how the two types of transient dynamics can arise from the phase space structure. The key point is how the trajectories connect the two fixed points. For small selection coefficient s , the change in the environment between the two fixed points is small; there is no significant process of equilibration with the environment taking place, just a substitution of cell types, and the trajectories starting in the vicinity of the sub-dominant population are almost straight. By contrast for large s the trajectories are seen to be curved and can be approximated by two straight lines.

We define the frequency takeover time by determining a threshold on the ratio of the invading vs. resident species. Writing the equations for the population densities as follows

$$\begin{aligned} \frac{du}{u} &= \frac{d}{dt} \ln u = \mu(\zeta) - 1 \\ \frac{dv}{v} &= \frac{d}{dt} \ln v = s\mu(\zeta) - 1. \end{aligned} \tag{B.4}$$

And defining a new variable

$$y = s \ln u - \ln v. \tag{B.5}$$

It is found that y obeys a simple differential equation with the following linear solution

$$y(t) = y(0) - (s - 1)t. \tag{B.6}$$

Now setting thresholds θ_i on the ratio of the invading population at the start of the process (e.g. $v(0) = \theta_i u^*$, $u(0) = 1 - \theta_i u^*$) and θ_f at the end of takeover t_{freq} (e.g. $u(t_{\text{freq}}) = (1 - \theta_f)v^*$, $v(t_{\text{freq}}) = \theta_f v^*$), one finds the frequency takeover time t_{freq} to be as in Eq. (4) in the main text.

One may expect that the takeover time will become shorter as the selection coefficient becomes large. This is indeed the case for takeover dynamics in an open unlimited environment (see Fig. 2). However, it is seen from Eq. (4) that the frequency takeover is in fact bounded from below as s increases. It will become clear in what follows, that a large selection coefficient drives a faster equilibration between the total population and the environment, but still the chemostat time scale places a bound on the inter-species equilibration process.

For an estimate of the density takeover time t_{dens} , we note that for large s the trajectories are approximately composed of two linear segments. In the first, the total environment changes significantly and reaches near its equilibrium value. In the second, the environment is almost constant, as seen by the

coordinate ζ , which changes very little in this segment. We use this observation to compute the two timescales separately.

The computation relies once again on Eqs. (B.5), (B.6), however the values of u and v at the time t_{dens} will be taken from crossover point between the two approximately linear segments in Fig. B.1. These trajectories are shown in their projection on the (u, v) plane in Fig. B.1(c). Starting from the vicinity of the unstable fixed point with an initial fraction θ_i , namely at the point whose coordinates are $(\zeta^*, u^*(1 - \theta_i), u^*\theta_i)$, and moving along the direction of the eigenvalue $(1 - \eta_2, -\eta_1, \eta_1 + \eta_2 - 1)$, the projection of this segment on the ζ -axis is simply the change in equilibrium value of the limiting nutrient, $\Delta\zeta^*$. The corresponding projections on the u and v axes are

$$\begin{aligned} \Delta u &= \Delta\zeta^* \left(\frac{-\eta_1}{1 - \eta_2} \right) \\ \Delta v &= \Delta\zeta^* \left(\frac{\eta_1 + \eta_2 - 1}{1 - \eta_2} \right). \end{aligned} \tag{B.7}$$

Adding these segments to the initial point in phase space gives the final values for u and v at the final point; inserting this into Eq. (B.6) gives the expression in Eq. (5) of the main text.

Appendix C. Two-state population in the chemostat with transitions

Here we present for completeness the linear stability analysis of Eq. (6) in the main text. Setting $\dot{u} = \dot{v} = 0$ one finds for the ratio of phenotypes at the fixed point $p = u^*/v^*$ satisfies a quadratic equation

$$\gamma_1 p^2 + [s(1 + \gamma_1) - (1 + \gamma_2)]p - s\gamma_2 = 0. \tag{C.1}$$

The solution of this equation $p = p(s, \gamma_1, \gamma_2)$ then determines completely the fixed point values. The fractions at the fixed point are $f_u = \frac{p}{p+1}, f_v = \frac{1}{p+1}$, which in turn determine the value of the resource through the relation

$$\frac{p}{p+1}\mu(\zeta^*) + \frac{1}{p+1}s\mu(\zeta^*) = \frac{p+s}{p+1}\mu(\zeta^*) = 1. \tag{C.2}$$

For a Monod growth function, one finds $\zeta^*(p) = \frac{\kappa}{\tilde{s}(p)\alpha - 1}$ with an effective α determined by the ratio: $\tilde{s}(p) = \frac{p+s}{p+1}$. The total population is then given by $u^* + v^* = 1 - \zeta^*$ and the fractions give the values of the individual values:

$$u^* = \frac{p}{p+1}(1 - \zeta^*(p)), \quad v^* = \frac{1}{p+1}(1 - \zeta^*(p)). \tag{C.3}$$

These equations define the only two fixed point of the system as $(1, 0, 0)$ and (ζ^*, u^*, v^*) with all nonzero values and $\zeta^* + u^* + v^* = 1$. Fig. C.1 shows the phase space for two values of $\gamma_1 = \gamma_2 = \gamma$. For $\gamma \ll 1$ (Fig. C.1(b)), the ghost of the unstable fixed point (*) corresponding to $\gamma = 0$ pulls the trajectories before they are attracted to the true fixed point, which is very close to mutual exclusion (the boundary of the manifold $\zeta^* + u^* + v^* = 1$). It is seen that also here the eigenvector on the manifold is approximately parallel to the line $u^* + v^* = \text{const}$, indicating that the total population and resource may equilibrate before the steady-state ratio between the two types relaxes.

To estimate the takeover time in the fluctuating environment, we note that in a slowly varying environment the most important factor affecting this transient is the initial condition, i.e. the (approximately steady state) fraction of unfit cells upon environment change. Since this term is dominant in the regime of small transition rates, we will neglect the effect of transitions and estimate the takeover time from competition alone.

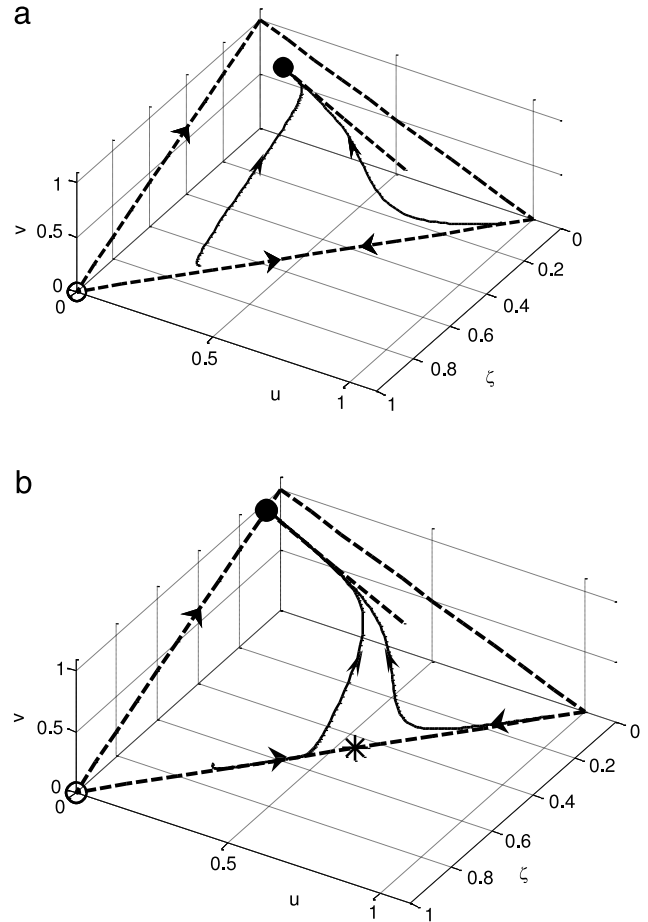


Fig. C.1. Phase space trajectories for the two-state population in the chemostat with transitions. Empty circles: trivial fixed point. Full circles: coexistent state. As transition rates decrease towards zero, a bifurcation is approached. The ghost of the unstable mutual exclusion state (plotted in panel b as a star) attracts the trajectories for a long period of time before they are finally attracted to the true fixed point. Parameters: $\alpha_1 = 1.2, \kappa = 0.1, s = 2, \gamma = 10^{-1}$ (a), $\gamma = 10^{-5}$ (b). Trajectories with the same initial conditions are plotted for comparison between (a) and (b).

Using once again Eqs. (B.5) and (B.6), we approximate the initial and final conditions by those computed above for the steady states:

$$\begin{aligned} y(0) &= s \ln u(0) - \ln v(0) \\ &= s \ln \left[\frac{1}{p+1} (u^* + v^*) \right] - \ln \left[\frac{p}{p+1} (u^* + v^*) \right] \\ y(t_{ik}) &= s \ln u(0) - \ln v(0) \\ &= s \ln \left[\frac{p}{p+1} (u^* + v^*) \right] - \ln \left[\frac{1}{p+1} (u^* + v^*) \right]. \end{aligned}$$

Solving these equations one finds the expression (12) in the main text.

References

Assmusen, M.A., Feldman, M.W., 1977. Density-dependent selection I. A stable feasible equilibrium may not be attainable. *Journal of Theoretical Biology* 64, 603–618.

Boyce, M.S., 1984. Restitution of r - and k -selection as a model of density-dependent natural selection. *Annual Review of Ecology, Evolution, and Systematics* 15, 427–447.

Cohen, D., 1966. Optimizing reproduction in a randomly varying environment. *Journal of Theoretical Biology* 12, 119–129.

Cooper, W., Kaplan, R.H., 1982. Adaptive “coin flipping”: a decision-tree examination of natural selection for random individual variation. *Journal of Theoretical Biology* 94, 135–151.

Desai, M.M., Fisher, D.S., 2007. Beneficial mutation–selection balance and the effect of linkage on positive selection. *Genetics* 176, 1759–1798.

Diekmann, O., 2003. A beginner’s guide to adaptive dynamics. *Banach Center Publications* 63, 47–86.

- Donaldson-Matasci, M.C., Lachmann, M., et al., 2008. Phenotypic diversity as an adaptation to environmental uncertainty. *Evolutionary Ecology Research* 10, 493–515.
- Dunham, M.J., Badrane, H., et al., 2002. Characteristic genome rearrangements in experimental evolution of *S. Cerevisiae*. *Proceedings of the National Academy of Sciences of the United States of America* 99 (25), 16144–16149.
- Elhanati, Yl., Schuster, S., Brenner, N., 2011. Dynamic modeling of cooperative protein secretion in microorganism populations. *Theoretical Population Biology* 80, 49–63.
- Gillespie, J.H., 2004. *Population Genetics: A Concise Guide*. The Johns Hopkins University Press, Baltimore.
- Hajji, M.E., Rapaport, A., 2009. Practical coexistence of two species in the chemostat—a slow-fast characterization. *Mathematical Biosciences* 218, 33–39.
- Jablonka, E., Oborny, B., et al., 1995. The adaptive advantage of phenotypic memory in changing environments. *Proceedings of the Royal Society of London Series B* 350, 133–141.
- Kussell, E., Kishony, R., et al., 2005. Bacterial persistence: a model for survival in changing environments. *Genetics* 169, 1807–1814.
- Kussell, E., Leibler, S., 2005. Phenotypic diversity, population growth and information in fluctuating environments. *Science* 309, 2075–2078.
- Lachmann, M., Jablonka, E., 1996. The inheritance of phenotypes: an adaptation to fluctuating environment. *Journal of Theoretical Biology* 181, 1–9.
- Lenormand, T., Roze, D., et al., 2008. Stochasticity in evolution. *Trends in Ecology and Evolution* 24, 157–165.
- Levins, R., 1968. *Evolution in Changing Environments*. Princeton University Press.
- Lord, P.G., Wheals, A.E., 1980. Asymmetrical division of *S. Cerevisiae*. *Journal of Bacteriology* 142 (3), 808–818.
- Meyers, L.A., Bull, J.J., 2002. Fighting change with change: adaptive variation in an uncertain world. *Trends in Ecology and Evolution* 17, 551–557.
- Mueller, L.D., 1997. Theoretical and empirical examination of density-dependent selection. *Annual Review of Ecology and Systematics* 28, 269–288.
- Rando, O.J., Verstrepen, K.J., 2007. Timescale of genetic and epigenetic inheritance. *Cell* 125, 655–668.
- Schuetz, R., Kuepfer, L., et al., 2007. Systematic evaluation of objective functions for predicting intracellular fluxes in *E. Coli*. *Molecular Systems Biology* 3 (119), 1–15.
- Sigal, A., Milo, R., et al., 2006. Variability and memory of protein levels in human cells. *Nature* 444, 643–646.
- Simons, A.M., 2011. Modes of response to environmental change and the elusive empirical evidence for bet hedging. *Proceedings of the Royal Society of London Series B* 278, 1601–1609.
- Smith, H.L., Waltman, P., 1995. *The Theory of the Chemostat: Dynamics of Microbial Competition*. Cambridge University Press, Cambridge.
- Stern, S., Dror, T., et al., 2007. Genome-wide transcriptional plasticity underlies cellular adaptation to novel challenge. *Molecular Systems Biology* 3, 106.
- Stolovicki, E., Dror, T., et al., 2006. Synthetic gene-recruitment reveals adaptive reprogramming of gene regulation in yeast. *Genetics* 173, 75–85.
- Thattai, M., van Oudenaarden, A., 2004. Stochastic gene expression in fluctuating environments. *Genetics* 167, 523.
- Veening, J.W., Smits, W.K., et al., 2008. Bistability, epigenetics and get-hedging in bacteria. *Annual Review of Microbiology* 62, 193–210.
- Wolf, D.M., Vazirani, V.V., et al., 2005. Diversity in times of adversity: probabilistic strategies in microbial survival games. *Journal of Theoretical Biology* 234 (2), 227–253.